Molecular Dynamics of Host−Guest Complexes of Small Gas Molecules with Calix[4]arenes

John E. Adams,* Jack R. Cox, Andrew J. Christiano, and Carol A. Deakyne

Department of Chemistry, University of Missouri−Columbia, Columbia, Missouri 65211-7600

Received: January 17, 2008; Revised Manuscript Received: May 19, 2008

The unexpected sorption of gases by a low-density *p-tert*-butylcalix[4]arene crystal polymorph raises fundamental questions about differential gas transport and sequestration in the organic solid state. To gain insight into the processes underlying these observations, we have used molecular dynamics simulations, augmented with calculations of potentials of mean force, to investigate the stability of isolated host−guest complexes and the relationship between the dynamics of these complexes and the dynamics of a solvated host molecule. Thermal fluctuations of the calixarenes themselves are found to be consistent with proposed mechanisms for gas entry into the host cavities, while relative host−guest stabilities correlate well with experimental absorption−desorption isotherms in some cases (CO_2 and CH_4) but not in others (C_2H_2). In these isolated systems, stable complexes characteristically form when the attractive interactions of the guest with the ring of negative charge density on the inner surface of the host cavity are not disrupted by thermal motion. The experimentally observed efficient uptake of gases such as C_2H_2 by the host crystals suggests, however, that stabilization of host−guest complexes in some systems may derive from dynamical constraints imposed by the crystal lattice.

I. Introduction

The serendipitous discovery that certain crystalline organic materials absorb small gas molecules under mild conditions of temperature and pressure has spurred an interest in these materials as gas storage and separation media.[1–12] Unlike zeolites or coordination networks that are characterized by well-defined gas transport channels, these organic crystals exhibit no such absorption pathways. Indeed, the real surprise is not that they absorb large volumes of small molecular gases, but rather that they absorb any gas at all. Most notable here is the low-density β_0 polymorph of *p-tert*-butylcalix[4]arene (TBC4; see Figure 1),[13–15] the porosity of which has been attributed to the formation of complexes in which gas molecules occupy extended cavities formed by face-to-face, although somewhat offset, calixarene hosts.[1,2,10,11,16] An ability to sequester gases within these cup-shaped host cavities, of course, does not alone explain the passage of gases through the crystals; the actual gas diffusion is thought to be facilitated by rotations of the *tert*-butyl groups such that entry into the voids is "gated".[3]

Seminal work on the porosity of TBC4 crystals has emerged from the Atwood group,[1–11] whose sorption isotherms indicate that gas sequestration can be efficient yet selective. For example, they have shown that acetylene can be absorbed at 1 atm ambient pressure and room temperature to densities beyond that at which the gas normally can be stored safely.[6] On the other hand, the preference for retention of CO_2 over H_2 when the crystal is exposed to a mixture of those gases at pressures less than 3 atm is sufficiently strong that they can be separated quantitatively.[2] Confounding the picture of the absorption process, though, is the difficulty of locating the sorbed gases within the host crystals. X-ray crystallography provides a check on whether gas absorption alters the crystal structure of the hosts, but frequently it does not resolve the guest positions, yielding instead only a suggestion of excess electron density within the host cavities.[2] NMR measurements yielding host-induced resonance frequency shifts[6,8,17] may not clarify the situation entirely either; detection of the guest gas within the crystal is not equivalent to unambiguous localization of the guests within the host cavities. Thus, there remains a critical need to characterize the dynamics of gases absorbed by these seemingly nonporous organic solids, to understand the preferential binding of certain gases within the host cavities, and to determine how the dynamics of the host species themselves alter the behavior of the guests.

Although the detailed dynamical characterization of calixarene hosts and their guests remains elusive, by no means have these systems been ignored entirely.[18–26] As an example of the investigations conducted to date, we note the calculation of the isomerization rates, both in the gas phase and in chloroform solution, of calix[4]arene[27] (C4) and TBC4[28] between their respective cone conformations and the higher-energy structures in which one or more of the aryl rings are rotated with respect to the others. The free energy barriers for these interconversions were estimated experimentally to be in excess of 40 kJ/mol, requiring the use of special sampling techniques to overcome the problems inherent in modeling processes that are rare events on the picosecond-to-nanosecond time scale accessible to conventional simulations. More extensive are the simulations of calixarene complexation in solution that are directed at optimizing guest binding and, in particular, guest binding selectivity, the application being chromatographic separation of a mixture of potential guest species. Here the work of Wipff and co-workers[29–35] is especially noteworthy. Other groups also have focused on the determination of binding energetics, including the calculation of free energies as a function of the distance between the centers of mass of the host and guest species.[36–42] The recent work by Dang and co-workers,[42] who compared the binding of CO_2 and H_2 to TBC4 in an effort to understand the selectivity of gas sequestration in the solid-state system, is particularly relevant to our present investigations.

* To whom correspondence should be addressed. E-mail: adamsje@missouri.edu.

10.1021/jp800492y CCC: $40.75
Published on Web 07/02/2008

Direct simulation of solid-state systems, either those involving calixarenes or others formed from related species (clathrates, for example), has received considerably less attention, however. A study by Alavi et al.[43] of inclusion compounds formed in the low-density β_0 polymorph of TBC4 yielded estimates of inclusion energies and of the frequencies of periodic motion executed by sequestered small gas molecules but did not address the consequences of the intramolecular dynamics of the hosts themselves. That group subsequently extended their previous work to an evaluation of the variation of inclusion energies as a function of cavity occupancy and identified nonlinearities in the trends when guest concentrations exceed those yielding 1:1 host−guest complex formation.[44]

In the present work, we step back and examine in greater detail the intramolecular and intermolecular dynamics of calixarene-guest complexes for a variety of small neutral molecular guests, focusing primarily on those for which uptake by crystalline TBC4 already has been demonstrated. Of particular importance to us are the differences observed in the structures and dynamics of complexes formed from closely related species. For example, we have examined complexes of CO_2 with C4, methylcalix[4]arene (MC4), and TBC4 in an attempt to identify those features of the host that are most important for guest retention. Conversely, we have carried out simulations of TBC4 complexes with ethane, ethylene, and acetylene to assess the likelihood that ethane and ethylene can be sequestered within a TBC4 crystal given the reported efficient uptake and retention of acetylene in this system. Finally, because methanol is a possible solvent for the calix[4]arenes being considered,[45] we have investigated the dynamics of methanol molecules bound to C4, to MC4, and to TBC4 as well as the dynamics of TBC4 immersed in liquid methanol. This last investigation also permits an evaluation of whether our isolated cluster simulations can provide useful insight into the dynamics of host−guest complexes in condensed phases.

II. Computational Methodology

All classical molecular dynamics simulations reported herein have been carried out using the AMBER 9 molecular dynamics package,[46] which implements the AMBER force field.[47,48] We have adopted the *gaff* force field parameters[49,50] for all species save for methanol, the parameters for which were taken from the *ff03* parametrization[51] for consistency with the optimized methanol solvent description that is included with AMBER 9. Bond lengths involving hydrogen atoms were routinely constrained by imposition of the SHAKE algorithm.[52] Problematic in any MD study based on a classical force field that includes atom-centered electrostatic interactions is the choice of partial atomic charges, given that there is no unique way to establish the values of these charges and that different commonly adopted procedures for determining the charges can yield quite different values. Because the AMBER force field itself was parametrized using RESP partial charges[53,54] determined by a two-stage fitting to the electrostatic potential given by HF/6-31G(d) ab initio calculations, we have adopted that procedure for fixing the charges in our systems. The GAUSSIAN 03 program[55] was used in determining these electrostatic potentials subsequent to optimizing the structures of the molecules at this same computational level. (For each system, a "tight" optimization was performed and frequencies were calculated to ensure that the structure described a potential energy minimum. Methanol again was handled differently; the RESP partial charges already provided in AMBER 9[46] were used without further adjustment.)

We began our simulations of the isolated hosts and host−guest complexes by equilibrating the systems at a temperature of 298 K (an NVT simulation based on Langevin dynamics[56] with a 5.0 ps^{-1} collision frequency) for 5×10^5 time steps of 1.0 fs each. Dynamical information was then collected from NVE simulations consisting of $5 \times 10^5 - 1 \times 10^6$ steps, again of 1.0 fs, with the coordinates of the systems being stored at intervals of 0.1 ps for subsequent analysis. For these isolated complex simulations, nonbonded potential contributions were cut off at a distance (4.0 nm) larger than the sizes of the systems themselves. In the case of the simulation of TBC4 in solution, we began by surrounding the single host molecule by 453 methanol molecules and imposing rectangular periodic boundary conditions. Long-range interactions in this extended system were determined by means of the Particle Mesh Ewald method,[57,58] with truncation of the direct-space sum at a distance of 0.80 nm. Here we began with a shorter (2×10^4 steps) NVT equilibration that was followed by an NPT equilibration (298 K, 1.0 bar) for an additional 5×10^5 time steps. The solution density obtained from this equilibration sequence is 0.81 ± 0.04 g cm^{-3}, a value that agrees well with the experimental result for pure methanol[59] of 0.79 g cm^{-3}. Finally, a constant-energy simulation, analogous with those performed for the isolated-complex systems, was carried out to generate the coordinate sets used in the analyses of the dynamics.

To aid our interpretation of the dynamical results, we also generated potentials of mean force (PMFs; i.e., free energies, ΔA, evaluated along defined reaction coordinates) for the removal of the guest molecule from the host cavity.[60,61] Umbrella sampling of the reaction coordinate, taken here to be the distance between the center of mass of the guest and the center of mass of the four phenolic carbons of the host, was carried out at 0.05 nm intervals over the range 0.15−0.90 nm with a biasing harmonic force constant of 8.386 kJ mol^{-1}. (This value incorporates the factor of 1/2 appearing in the usual expression for a harmonic biasing potential, that is, it conforms to the AMBER force definition convention.) For each position of the biasing potential minimum, the system was equilibrated for 100 ps (again with a time step of 0.001 ps) prior to accumulating system configuration data at 0.01-ps intervals for a total of 2 ns. Application of the weighted histogram analysis method[62] (WHAM) to this accumulated data then yielded the desired free energy values. We carried out the WHAM calculations using the readily available Grossfield code[63] with a bin size of 0.01 nm and a convergence tolerance of 1×10^{-6}; error bars were obtained by invoking the Monte Carlo bootstrap error analysis incorporated in that code with 50 Monte Carlo trials. Finally, because comparing free energies determined for different host−guest complexes requires that we have a common reference state, our reported free energies have been shifted so that their asymptotic values plateau at zero.

III. Complexes Involving Small Hosts: Calix[4]arene and Methylcalix[4]arene

A. Calix[4]arene. Although our special interest in this work lies in the dynamics of TBC4, that being the species that has displayed such remarkable porosity in the solid state, we begin our discussion here with the simplest host molecule, C4. Of all the host molecules considered, C4 is characterized by the shallowest cavity, that is, the shortest distance between the lower rim of the cavity (the narrow end of the "cone" where the OH groups are bound) and the upper rim (the end of the cone where the substituent groups, here just hydrogens, are bound). Two significant dynamical features of this molecule, features found to be equally characteristic of the other host species examined, emerge from our simulations. First, as others have suggested

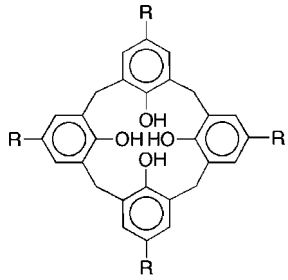

Figure 1. Calix[4]arenes.

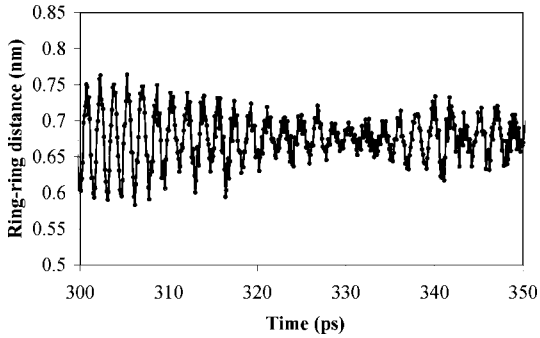

Figure 2. Oscillation of "facing" aryl rings in C4 at 298 K. The distribution of distances between the ring centers over the entire 500 ps simulation is characterized by an average distance of 0.68 nm and a standard deviation of 0.04 nm.

previously, the OH groups at the lower rim are effectively locked in an eight-membered, hydrogen-bonded ring. Over the simulation times considered here (roughly 2 ns), we find no evidence for the rotation about a carbon−oxygen bond that would lead to a hydrogen flipping between interactions with neighboring oxygen atoms. We would not expect this rotation to occur under the conditions of our simulation because it would involve a simultaneous, or nearly simultaneous, movement of all the lower-rim hydrogens, but nonetheless it is important to note the rigidity of this hydrogen bond network even in the absence of explicit hydrogen-bond potential terms in the AMBER force field.[47,48]

The second important feature of C4 dynamics is the large-amplitude oscillatory motion of the four aryl rings. These rings exhibit an asymmetric breathing mode in which the two aryl rings facing one another across the cavity move inward and outward synchronously, the motion of adjacent rings being comparable but 180° out of phase. A time slice of the simulation for one of the pairs of facing aryl rings is shown in Figure 2.

The amplitude of these oscillations is seen to vary as energy flows through the molecule (the greatest deviations from the equilibrium distance between the centers of the facing rings are found to be quite substantial, at 0.13 nm), but the frequency of the oscillations is reasonably constant at about 20 cm^{-1}. This value is consistent with the 11.5 cm^{-1} harmonic frequency for this mode predicted by the ab initio calculation from which the RESP partial atomic charges[53,54] were derived for this system.

To undertand why certain guests would form stable host−guest complexes with C4 and to gain insight into the structures that might derive from complexation, we also have examined the electrostatic environment within the C4 cavity. In Figure 3, we give electrostatic potential maps[64] calculated at the HF/6-31G(d) level (the same calculational level at which the RESP partial charges[53,54] were fit).

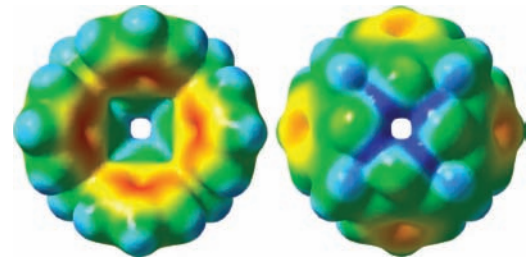

Figure 3. Two views of the electrostatic potential map of C4 determined at the HF/6-31G(d) level. (The electrostatic potential here is mapped onto the surface of constant total electron density at 0.005.) The view on the left shows the host cavity, while the view on the right is of the lower rim of the calixarene as seen from the "outside". Here the most negative net charge is shown in red; the most positive net charge is shown in blue.

Note that the inner surface of the host cavity shows a significant excess negative charge density just where one would expect to find the π electrons of the aryl rings and that a band of negative charge therefore lines the cavity. In addition, there is an asymmetry in the distribution of excess negative charge associated with the π electrons such that the negative charge density is somewhat greater on the inside surface of the calixarene than it is on the outside surface. The presence of this asymmetry, coupled with the constructive overlap of regions of negative charge density within the cavity, suggests that entry of a positively charged species into the cavity will be energetically favored irrespective of whether that entry is facilitated by the dynamics of the host. Note also in these electrostatic potential maps that the hydroxyl groups at the lower rim of the calixarene do not generate a region of net negative charge within the cavity. Indeed, the negative partial charges on the oxygen atoms of these groups are essentially buried in the overall net positive charge contributed by the hydroxyl hydrogens and the hydrogens of the methylene bridges, with the highest net positive charge density appearing on the exterior surface of the molecule.

For our characterization of the dynamics of isolated host−guest complexes involving C4, we selected carbon dioxide and methanol as our guest molecules of interest because they are expected to interact quite differently with the electrostatic environment of the host cavity. Carbon dioxide is nonpolar, although it is better described as nondipolar due to its appreciable quadrupole moment,[65] while methanol is polar and capable of forming hydrogen bonds. We were not able to equilibrate a C4/CO_2 complex at 298 K; the guest molecule escaped from the cavity during the NVT equilibration phase of the simulation. Complexes formed at 100 and 200 K, however, are stable over the nanosecond time scale of the simulation. At both temperatures, the preferred orientation of the CO_2 guest molecule is with its C_s symmetry axis aligned parallel with the C_4 axis of the C4 host. This preferential orientation is seen clearly in a plot (Figure 4) of the distance of the guest atoms from what, for convenience, we will term henceforth the "C-base point" of the host. The C-base point is defined here as the center of mass of the four carbon atoms to which the OH groups of the lower rim are connected. (Not coincidentally, this is the same point noted in Section II in defining a reaction coordinate for the calculation of potentials of mean force.) On only one occasion over the 500 ps simulation does the CO_2 rotate such that its symmetry axis is perpendicular to the C_4 symmetry axis of the host, and even then the molecule rotates back to its original orientation without switching the positions of the oxygen atoms. The results obtained at 100 K are qualitatively similar, however the displacements of the guest atoms are smaller at the lower temperature.

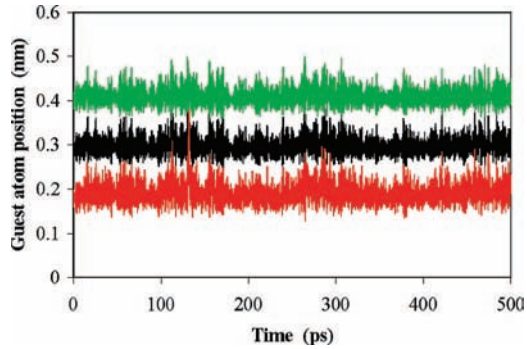

Figure 4. Distance of the carbon (black) and oxygen (red and green) atoms from the C-base point, defined in the text, in an isolated C4/CO_2 complex equilibrated at 200 K.

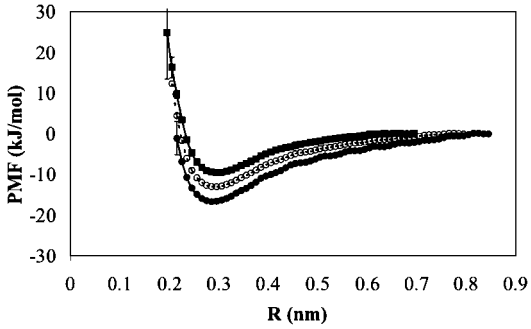

Figure 5. Potential of mean force for the removal of CO_2 from C4 at 100 (solid circles), 200 (open circles), and 298 K (solid squares). Error bars correspond to the Monte Carlo bootstrap estimates cited in the text and are within the dimensions of the plotting symbols unless otherwise indicated.

(The standard deviations for the distributions of distances are 22−28% smaller at 100 K, with the greatest effect being on the displacement of the oxygen atom nearest the C-base point.)

Of course, one might expect the CO_2 guest to adopt the observed orientation on the basis of the reported geometry of a benzene/CO_2 gas-phase cluster. Bernstein and co-workers[66] determined spectroscopically that CO_2 prefers to bind with carbon lying along the C_6 rotation axis of benzene and with the carbon−oxygen bonds oriented parallel to the plane of the benzene ring. (The binding energy in that case was found to be 10.3 kJ mol^{-1}.) Maximization of the guest-aryl ring interaction for a C4 host thus should yield a propensity for CO_2 to sit "on end" in the calixarene cavity, the structure that indeed is observed in our simulations. Note also that the equilibrium intermolecular distance determined for a benzene/CO_2 cluster is 0.327 nm, which is only 0.01 nm less than half the equilibrium distance between the centers of the facing aryl rings in an isolated C4 molecule (Figure 2). This guest orientation is furthermore consistent with the electrostatic potential maps of Figure 3: the carbon atom, bearing a positive partial charge, is localized in the region of the negative charge band of C4, while the relatively negative oxygen atoms are found in the cavity where the charge density is neutral or positive.

Insight into why CO_2 is not retained by an isolated C4 host at room temperature derives from the calculation of temperature-dependent PMFs along the reaction path defined by the distance between the C-base point of the host and the center of mass of the guest. The resulting curves, determined for the same three temperatures at which the dynamics was studied, are shown in Figure 5.

Although these three curves share a common shape, the magnitude of the free energy of binding not only decreases with increasing temperature, the range of R values over which the magnitude of ΔA is non-negligible narrows markedly. Accordingly, the larger thermal fluctuations that characterize the dynamics of the guest at the higher temperature greatly increase the likelihood that the guest will be lost from the host cavity. The minima in these free energy curves are given in Table 1, along with estimates of binding internal energies and entropies along the reaction coordinate obtained by fitting the free energy data to the equation $\Delta A = \Delta U - T\Delta S$ and assuming no temperature dependence of ΔU and ΔS themselves. Note that the binding energy determined in this way is twice that reported by Bernstein and co-workers for a gas-phase benzene·CO_2 cluster. Perhaps of more interest, though, is ΔS, which is more negative for this system than for most of the others studied and, in particular, is more negative than for CO_2 sequestered by the other hosts. (We shall return to this latter point below.) This result suggests that for CO_2 to be retained within the C4 cavity, its motion must be severely restricted, this inferred restriction being consistent with our observation that no end-over-end rotation of the guest occurs in those simulations in which the guest is retained.

Unlike carbon dioxide, methanol is found to form a stable complex with C4 at room temperature. The preferred orientation of the guest molecule in this case is with the methyl group toward the lower rim of the host and with the carbon−oxygen bond tilted with respect to the C_4 symmetry axis of C4. To quantify this orientation preference, we extracted the angle

TABLE 1: Thermodynamic Parameters Evaluated along a Reaction Coordinate for Loss of the Guest from the Host Cavity

host	guest	T (K)	ΔA (kJ mol^{-1})[a]	ΔU (kJ mol^{-1})[b]	ΔS (J mol^{-1} K^{-1})[b]
C4	CO_2	100	−16.7		
		200	−13.1	−20.3	−36.1
		298	−9.6		
	MeOH	100	−15.8		
		200	−11.3	−19.7	−40.8
		298	−7.7		
MC4	CO_2	100	−17.5		
		200	−14.2	−20.7	−32.0
		298	−11.1		
	MeOH	100	−15.7		
		200	−12.5	−19.3	−34.5
		298	−8.9		
TBC4	CO_2	100	−19.0		
		200	−16.3	−21.4	−24.8
		298	−14.1		
	MeOH	100	−20.5		
		200	−17.4	−23.6	−31.6
		298	−14.2		
	CH_4	100	−9.9		
		200	−8.3	−11.7	−17.3
		298	−6.5		
	C_2H_2	100	−10.9		
		200	−8.4	−13.2	−23.7
		298	−6.2		
	C_2H_4	100	−12.0		
		200	−8.9	−14.9	−29.5
		298	−6.2		
	C_2H_6	100	−14.0		
		200	−10.4	−16.6	−28.3
		298	−8.4		

[a] Uncertainties of 0.1−0.2 kJ mol^{-1} are estimated from a Monte Carlo bootstrap analysis using 50 trials. [b] Linear least-squares fit uncertainties are 0.3 and 1.4 J mol^{-1} K^{-1} for ΔU and ΔS, respectively, determined assuming a uniform uncertainty of 0.2 kJ mol^{-1} in ΔA.

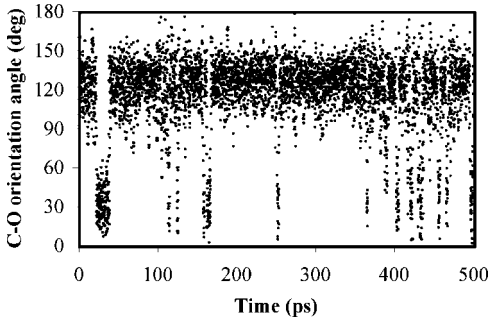

Figure 6. Carbon−oxygen bond orientation of a methanol guest in a C4 host at 298 K.

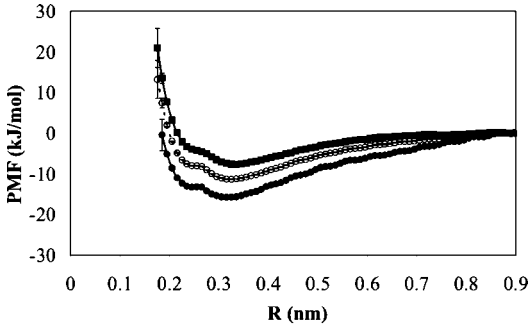

Figure 7. Potential of mean force for the removal of MeOH from C4 at 100 (solid circles), 200 (open circles), and 298 K (solid squares). Error bars have been determined using the method noted in Figure 5.

between a line joining the C-base point with the center of mass of the C−O bond and a line coincident with the C−O bond. The resulting distribution of angles, shown in Figure 6, has an average of 120° and a standard deviation of 27°, with the majority of the values lying between 100° and 150°.

This tilt angle is such that the O−H bond in MeOH is directed toward the negatively charged center of one of the aryl rings, the expected orientation if OH-π hydrogen bonding contributes significantly to the stability of the complex.[67] The MeOH molecule certainly is not static within the cavity; the hydrogen bond interaction shifts from one aryl ring to another. The occasional appearance of data points centered around 30° also reveals that the MeOH guest can invert its orientation within the cavity (in doing so, the hydrogen bonding can be maintained, although now the O−H bond is directed "upwards" toward an aryl ring rather than "downwards" toward that ring), but the relative lengths of time spent in the two orientations indicate that the orientation having the alcohol group of the guest at the upper rim of the host is energetically favored.

Calculated potentials of mean force for the C4/MeOH complex further corroborate this picture of two preferred guest orientations. In Figure 7, we find that the curves are characterized by two minima, one at about 0.32 nm corresponding to the orientation in which the oxygen atom is directed toward the (open) upper rim of the host and one at about 0.25 nm corresponding to the orientation in which the oxygen atom is directed toward the lower rim of the host. Indeed, the signature of a distinct preference for particular guest orientations emerges from the temperature dependence of the free energy, from which we derive a value of ΔS larger in magnitude than that found for any of the systems that we have examined (see Table 1). Note, too, that the relative free energies of these two guest orientations are entirely consistent with the preference for the former one (oxygen toward the upper rim) that is seen in the

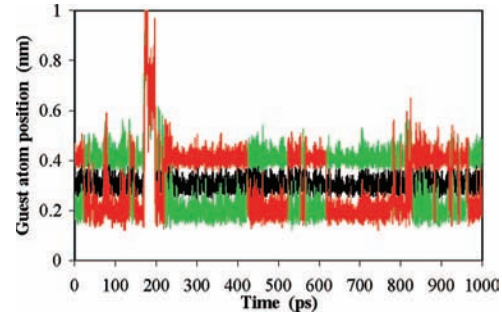

Figure 8. Distances of the carbon (in black) and oxygen (in red and green) atoms of CO_2 from the C-base point of MC4 at 298 K.

dynamics simulations. Deeper penetration of the guest molecule into the host cavity, though, is accommodated by orienting the oxygen toward the lower rim of the host and directing the methyl group toward the opposite open end of the cavity. The origin of this reorientation is easily identified from an examination of our electrostatic potential maps (Figure 3): the inner surface of the host bears a partial positive charge that leads to an attractive interaction with the oxygen atom but a repulsive interaction with the relatively positive methyl group.

Before leaving the discussion of the C4/MeOH complex, we note that formation of a host−guest complex with MeOH also perturbs the dynamics of C4. If we again examine the distances between the centers of the facing aryl rings, we do not find any difference in the average distances deriving from the presence of the guest. However, we do find that the asymmetric breathing vibrations of the aryl rings are damped, with the standard deviation of the distribution of distances dropping from 0.035 in isolated C4 to 0.026 in the complex (a reduction of 25%). Plots analogous to the one shown in Figure 2 also suggest that the guest disrupts the regular pattern of low-frequency host vibrations, affecting both the frequency pattern and the amplitude of the oscillations.

B. Methylcalix[4]arene. Methylcalix[4]arene presents an interesting comparison with C4 in that its cavity is deeper, and thus it has the potential for retaining a guest that might not be retained by C4. The dynamics of MC4 and C4 themselves do not differ greatly; they both are characterized by a rigid hydrogen bond network at the lower rim and a large-amplitude (relative to the other modes), low-frequency asymmetric breathing vibration, although in MC4 the frequency of that mode is reduced to $\sim$13 cm^{-1} as a consequence of the greater mass of the methyl-substituted aryl rings. We also find that MC4, like C4, forms a stable host−guest complex with methanol, one that is stabilized by attraction of the alcohol's OH group to the aryl rings.

Unlike C4, however, MC4 forms a complex at room temperature with carbon dioxide that survives on the nanosecond time scale, although our simulation suggests that the complex is by no means as robust as the one formed with methanol. In Figure 8, we give a plot similar to that shown in Figure 4, but for an MC4 host and a temperature of 298 K. Notable in this plot is direct evidence for rotation of the guest molecule within the host cavity, indicated by the interchange of the red and green curves. In C4, loss of the CO_2 guest appears to be associated with having sufficient kinetic energy to permit a rotation of the guest that momentarily disrupts the favorable interactions with one pair of the aryl rings. The somewhat deeper cavity of MC4 allows completion of the rotation and reestablishment of the optimal interaction orientation before the guest has enough time to leave the cavity entirely. The thermodynamic parameters in

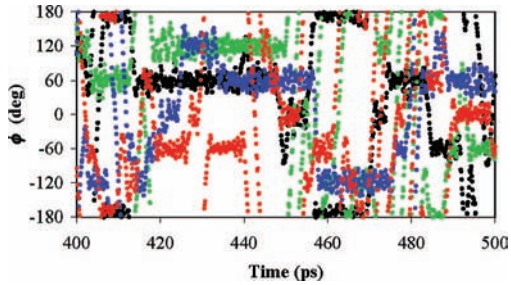

Figure 9. Dihedral angles for rotation of the four *tert*-butyl groups in TBC4 (298 K).

Table 1 also indicate that binding of CO_2 to MC4 is more favorable than is binding to C4, but of particular interest is the observation that the entropy associated with that binding is smaller in magnitude for the MC4/CO_2 complex. (The same relationship holds for the analogous MC4/MeOH complexes.) This result further attests to the opportunity for CO_2 to be more mobile within the MC4 host and yet still being retained.

The unusual feature appearing in Figure 8 at roughly 200 ps deserves special mention, though. This feature is attributable to the guest having just enough kinetic energy to escape from the host cavity but not enough energy to overcome the host−guest potential interactions entirely. As the CO_2 molecule slowly leaves the cavity, it becomes temporarily trapped at the face of an aryl ring on the *outer* surface of the calixarene. From there, it is able to move across the surface of the host until it encounters one of the gaps between the rings and reenters the cavity. We find only one instance of such an excursion during our nanosecond simulation, but finding even one on this time scale lends support to the model anticipated for sequestration of a gas by a solid-state host: the gas moves through interstices within the crystal lattice, interacts with the host species (initially with their outer surfaces, one presumes), and slips into a host cavity during a structural fluctuation of that host molecule.

IV. *p-tert*-Butylcalix[4]arene Complexes

We begin our discussion of TBC4-guest complexes with a characterization of the isolated host molecule. There is no qualitative difference between the dynamics observed for TBC4 and the results described above for C4 and MC4, although the expected quantitative differences indeed are seen. In particular, the increased masses of the substituents at the para positions of the four aryl rings lead to a reduction in the frequency of the characteristic asymmetric vibration to roughly 7 cm^{-1}, nearly a 50% decrease in the value observed for MC4 and a 70% decrease in the corresponding frequency found for C4. (The ring−ring distances, on the other hand, are not significantly different; the distribution of distances in isolated TBC4 has an average of 0.67 nm and a standard deviation of 0.04 nm.) More interesting is the dynamics of the *tert*-butyl groups themselves, which we follow here by defining a dihedral angle (ϕ) for each of the four groups that measures rotation about the C−C bond linking the central carbon of that group to the para carbon of the aryl ring to which the group is attached. The four calculated dihedral angles determined over a 100-ps time slice of a simulation of an isolated TBC4 molecule are shown in Figure 9.

In this plot, we find a definite propensity for the *tert*-butyl groups to be oriented at angles whose values are multiples of 60° in accordance with the 3-fold rotational symmetry of the substituent. Note, though, that any one preferred orientation persists for no longer than 30 ps, that persistence times of 10 ps or shorter are common, and that the data sets contain numerous examples of continuous rotations through 360° or more. These results lend credibility to the model for gas-molecule entry into solid-state host cavities suggested by Atwood and co-workers,[3] whereby rotations of the *tert*-butyl groups facilitate passage in and out of the calixarene cup. Of course, we presume that these rotations are damped to some extent in the more constrained environment presented by a crystal lattice, yet the facility with which they occur in the gas-phase species suggests that their motion may indeed contribute to the extraordinary porosity of crystalline TBC4.

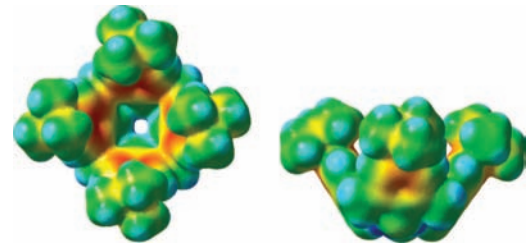

Figure 10. Electrostatic potential maps for TBC4. The left-hand view shows the host cavity; the right-hand view is of the "side" of the exterior of the molecule, obtained by rotating the left-hand view by 90°.

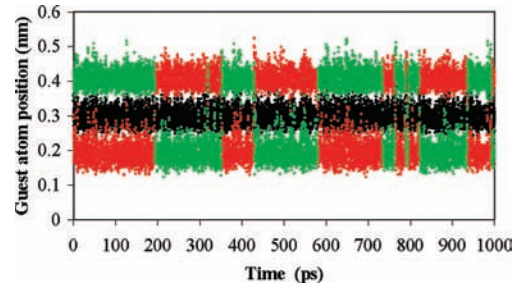

Figure 11. Distances of the carbon (in black) and oxygen (in red and green) atoms of CO_2 from the C-base point of TBC4 (298 K).

In characterizing host−guest complexes involving TBC4, we begin by examining the electrostatic potential presented by the host. Electrostatic potential maps[64] analogous to those of Figure 3 (including an identical color scale) are shown in Figure 10. (There is no significant difference between the electrostatic potential at the lower rim of TBC4 and what was found at the lower rim of C4, thus we omit that view here.)

In TBC4 as in C4, we find the interior of the cavity to be banded with a region of negative charge density. Away from that band, at the upper and lower rims, the charge density is neutral to positive, so that a positively charged guest will tend to be localized midway within the cavity. We also again find that the inner surface of the cavity bears a somewhat larger negative charge density than does the corresponding outer surface. Finally, the views of Figure 10 make it clear that the *tert*-butyl substituents both lengthen the host cavity and constrict the entry to it. This latter observation necessarily strengthens the case for examining the dynamics of this host molecule inasmuch as this constriction varies as the molecule vibrates and the substituents undergo internal rotations.

Given that CO_2 forms a stable complex with MC4 (although, perhaps, a fragile one) at room temperature, the even deeper host cavity afforded by TBC4 certainly should accommodate a CO_2 molecule under these conditions, and indeed we find that it does. The volume of this larger cavity is such that rotation of the guest can occur without jeopardizing the stability of the inclusion complex, a result that can be seen in Figure 11, where the time dependence of the positions of the atoms of the guest is depicted.

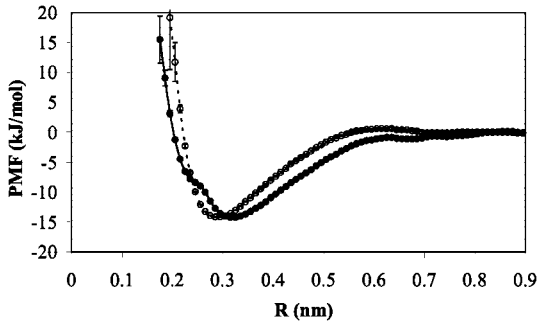

Figure 12. Potential of mean force for the removal of CO_2 (open circles) and MeOH (solid circles) from TBC4 at 298 K. Error bars have been determined using the method noted in Figure 5.

The calculated potentials of mean force for escape of the CO_2 guest attest to the stronger binding of the guest to the TBC4 host than to either C4 or MC4. Not only is the magnitude of the free energy greater for binding at the equilibrium complex geometry (Table 1), but the greater binding energy more than compensates for the greater mobility of the guest within the larger volume of the host cavity. (The magnitude of ΔS decreases by more than 30% for sequestration by a TBC4 host in comparison with a C4 host and by more than 20% in comparison with an MC4 host. Furthermore, the entropic contribution to the free energy decreases as the host cavity lengthens.) A change is also seen in the shape of the free energy curve along the reaction coordinate. In Figure 12, we give that curve (the open circles) for the TBC4/CO_2 complex, and we call attention here to the local maximum appearing at about 0.6 nm.

A snapshot of the system during the simulation for which the minimum in the umbrella sampling biasing potential was fixed at 0.6 nm reveals that this maximum in the free energy curve derives from the reorientation of the CO_2 molecule so that its bond axis lies perpendicular to the symmetry axis of the host. This reorientation enhances the attractive interaction between the oxygens of CO_2 and the relatively positive methyl groups of the *tert*-butyl substituents, but it does so at the price of constricting the opening through which the departing guest must pass. This same reorientation has been reported recently by Dang and co-workers[42] in a study of this same system that did not include the full dynamical effects incorporated here. (The magnitude of the equilibrium binding free energy reported by that group is somewhat larger than the value we report in Table 1, although their value appears to be quite comparable with our derived binding energy, ΔU.)

The effect of the guest on the dynamics of the host itself is also of interest. Although the width of the cavity remains unchanged at an average ring−ring distance of 0.67 nm, the low-frequency asymmetric breathing frequency of the host increases somewhat, to 11 cm^{-1}, and the amplitude of the oscillation drops as a consequence of the attractive interaction between the aryl rings and the guest molecule. (This reduction in the oscillation amplitude is reflected in a reduction in the standard deviation of the distribution of ring−ring distances to 0.03 nm.) Occupation of the host cavity by CO_2 does not impede, however, the rotation of the *tert*-butyl groups of the host. A plot of the dihedral angles characterizing that rotation is given in Figure 13, where one finds results very similar to those presented previously for the isolated host (Figure 9). Again, the periods over which the *tert*-butyl groups are (relatively) stationary tend to be about 10 ps in length, but rotation remains facile. This general characterization is entirely

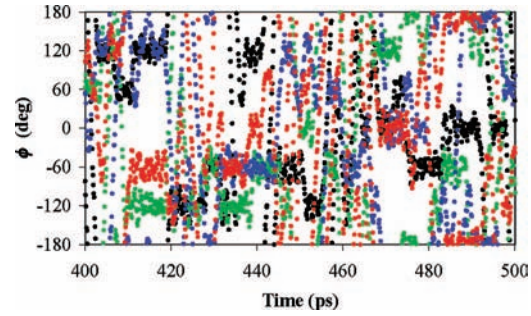

Figure 13. Dihedral angles for rotation of the *tert*-butyl subsituents in an isolated TBC4/CO_2 complex at 298 K.

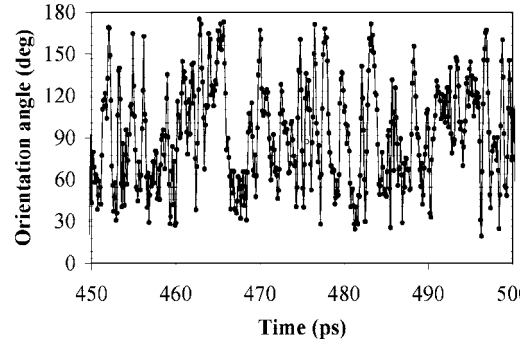

Figure 14. Orientation angle of methane sequestered in a TBC4 cavity at 100 K. The lines connecting the points are presented for ease in following the data sequence.

consistent with the observation that adsorption−desorption isotherms generated for CO_2 uptake by a low-density TBC4 crystal display no evidence of the hysteresis that might be expected if occupation of the host cavity were to restrict the rotation of the *tert*-butyl groups and thus to inhibit gas exit from the cavity.[6]

We turn now to a series of small hydrocarbon guests (CH_4, C_2H_6, C_2H_4, and C_2H_2). Of these, methane and acetylene are known to be sorbed readily by the β_0 TBC4 crystal polymorph,[3,6,8] and thus a systematic investigation of the series is warranted. We begin with methane. In an NVE simulation starting from the configuration given by an NVT simulation performed at 298 K, the methane guest does not remain sequestered within the TBC4 host cavity over a time period of 500 ps, but complexes are found at 100 and 200 K that persist at least to 1 ns. Even at the lowest of these temperatures, the methane molecule rotates very rapidly within the cavity, the seemingly erratic nature of this rotation being manifest in the time slice of the methane orientation angle depicted in Figure 14. (The orientation angle here is defined as the angle between a carbon−hydrogen bond in methane and a line that connects the methane carbon and a TBC4 aryl ring center. The data shown derive from an arbitrary choice of one of the four carbon−hydrogen bonds and one of the four aryl rings.)

Not only does the methane molecule rotate within the host cavity, it also translates within the cavity. Of particular interest to us is its motion in the direction leading to desorption, thus we have calculated the distance between the methane's carbon atom and the C-base point of TBC4. The distribution of distances obtained at 100 K is characterized by an average of 0.29 nm and a standard deviation of 0.023 nm, while the distribution at 200 K has an average of 0.31 nm and a standard deviation of 0.032 nm. As expected, increasing the temperature of the system leads to larger excursions of the guest away from its energetically most favorable binding position, although at

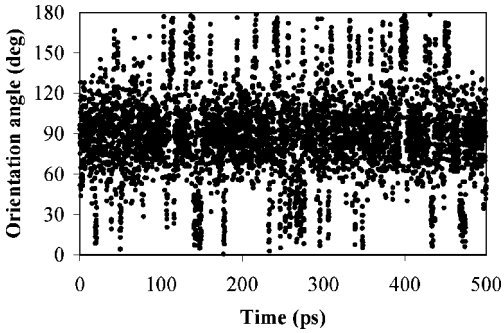

Figure 15. Orientation of acetylene within a TBC4 cavity at 200 K. Clustering of the angle around 90° indicates a propensity for the acetylene bond axis to lie perpendicular to the C_4 axis of TBC4.

temperatures less than or equal to 200 K that excursion remains small enough that methane stays within the cavity. More precisely, we should say that the excursion is small enough that the guest can avoid repulsive interactions with the *tert*-butyl moieties that would lead to ejection of the methane.

Compared with methane, the other hydrocarbon guests examined are far less spherical and so offer more opportunities for preferential bonding orientations. Neither acetylene nor ethylene were found to yield stable complexes at room temperature, even though acetylene has been shown to be retained readily in the solid state and to exhibit adsorption−desorption hysteresis suggestive of an attractive acetylene−host interaction.[6] Again, therefore, we concentrate on their dynamics at lower temperatures. In Figure 15, we give the time dependence of the orientation angle of acetylene, defined as the angle between a line extending from the C-base point of TBC4 to the midpoint of the acetylene's carbon−carbon bond and a line from that same bond midpoint to one of the acetylene hydrogens.

The preference for acetylene to lie perpendicular to the symmetry axis of the TBC4 cavity is consistent with previous studies indicating that the lowest-energy configuration of a benzene-acetylene cluster has the acetylene molecule coincident with the benzene's C_6 symmetry axis. Of course, such an orientation in the host cavity in the present case optimizes the interactions with one set of facing aryl rings (the relatively positive hydrogens of acetylene interacting with the negative partial charges centered on the ring centers) but yields less favorable interactions with the other two aryl rings.[68] Planar rotation of acetylene then exchanges the pair of aryl rings with which the interaction is strongest, so rotation parallel to the C-base plane is preferred in comparison with end-over-end rotation such as that observed for CO_2 in this environment.

Ethylene also lies "flat" within the TBC4 cavity (i.e., the plane of the molecule is parallel to the C-base plane of the host), especially at low temperatures. This preferred orientation is easily seen in the plot of dihedral angles given in Figure 16, where ϕ is a measure of the rotation of the guest about the C_4 symmetry axis of the host. (Note that the angle as defined "wraps around" at 180° and −180°.)

The values of 0°, ±90°, and ±180° all correspond to orientations in which the carbon−carbon bond of ethylene lies parallel to a line connecting the centers of facing aryl rings. Reorientations here are slow, generally on the order of hundreds of picoseconds, and rotations of ethylene about its long axis are quite infrequent. Increasing the system temperature to 200 K, however, yields quite different dynamics: reorientation of the guest becomes rapid, with relatively stable configurations surviving for only a few picoseconds. A time slice illustrating this enhanced mobility is given in Figure 17. While the preferred

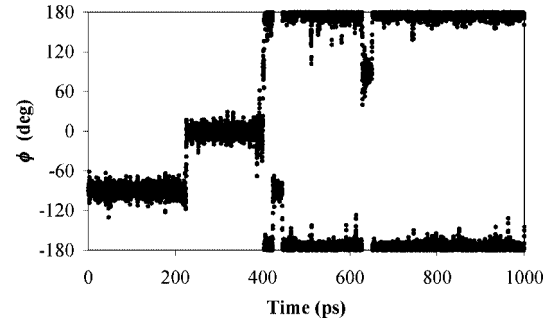

Figure 16. Orientation angle for ethylene within the cavity of TBC4 at 100 K.

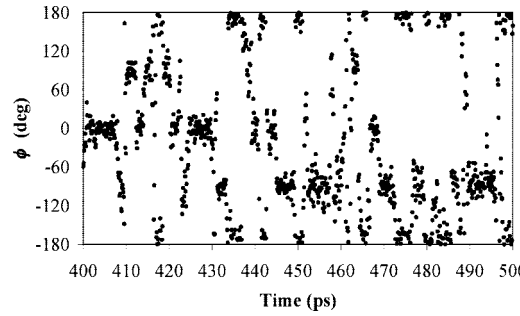

Figure 17. Orientation angle for ethylene within the cavity of TBC4 at 200 K.

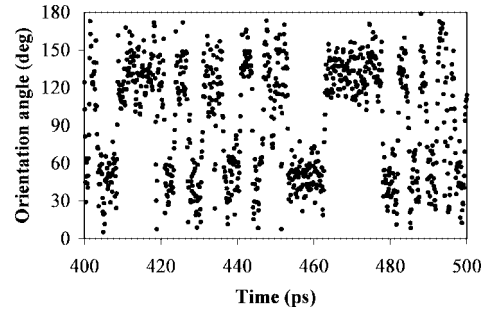

Figure 18. Orientation of the carbon−carbon bond of an ethane molecule complexed with TBC4 at 298 K.

orientations of ethylene clearly persist to the higher temperature (albeit with significantly truncated lifetimes), the large-amplitude oscillations of the guest about its long axis now are no longer rare.

Ethane, the least acidic of the hydrocarbons considered, might not be expected to form a stable complex with TBC4; the less positive partial charges on the individual hydrogens do not interact as strongly with the negatively charged ring centers. However, we do in fact find a TBC4/ethane complex to be stable at room temperature. To understand the source of this stability, we have examined the orientation of the ethane guest within the host cavity and have found that it fits within the cavity with its carbon−carbon bond axis tilted. This orientation preference is depicted in Figure 18, where the orientation angle plotted is defined in the same way as is the case of acetylene (Figure 15).

The preferred orientations of the carbon−carbon bond lie within two bands at 30−60° and 120−150°. These bands reflect the same orientation preference, of course; they differ only in which of the two carbon atoms is closer to the upper rim of the cavity. At these canted molecular orientations, the hydrogens of ethane are better positioned to interact directly with the aryl rings and to produce net attractive interactions strong enough to yield a stable room-temperature complex. By no means is

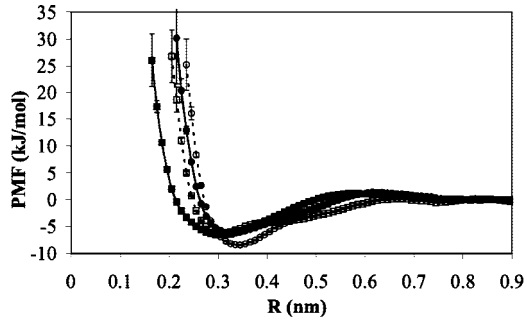

Figure 19. Potential of mean force for the removal of CH_4 (solid squares), C_2H_2 (open squares), C_2H_4 (solid circles), and C_2H_6 (solid circles) from TBC4 at 298 K. Error bars have been determined using the method noted in Figure 5.

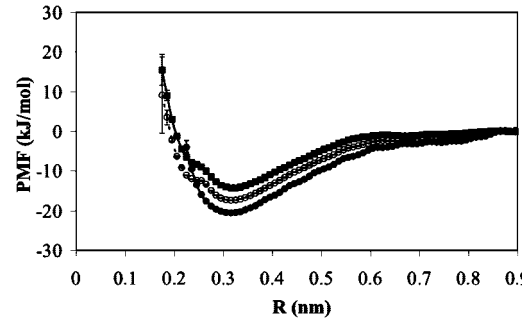

Figure 20. Potential of mean force for the removal of MeOH from TBC4 at 298 (solid squares), 200 (open circles), and 100 K (solid circles). Error bars have been determined using the method noted in Figure 5.

the guest locked into a specific orientation at this temperature, but rotation about the carbon−carbon bond allows the hydrogens to maintain their attractive interactions with the host as the ethane undergoes thermal motion within the cavity.

Given the dynamical differences observed for these hydrocarbon guests, we expect that differences also should appear in the calculated potentials of mean force for the host−guest complexes, and indeed such is the case. The free energy curves determined at 298 K are shown in Figure 19 and, again, the relevant thermodynamic quantities are summarized in Table 1.

Methane, acetylene, and ethylene exhibit very similar equilibrium binding free energies with TBC4 at 298 K, although this similarity obscures some significant differences in these systems. In particular, note that the magnitude of ΔS is particularly small for the CH_4 guest and thus is consistent with the facile rotation of that molecule that was observed in our simulations, whereas the larger magnitudes of ΔS associated with the other guests are consistent with the preferential binding orientations observed for those species. Note, too, that all these guests, save for acetylene, exhibit local free energy maxima in the vicinity of 0.6 nm, a distance roughly corresponding to passage of the guest through the opening at the upper rim of the host cavity, an opening that is dynamically constricted by the motion of the *tert*-butyl groups. Interactions between the hydrogens of the guest species and the *tert*-butyl hydrogens are repulsive, and thus the energy needed to escape from the cavity is somewhat greater than if the interactions were negligible. Indeed, that acetylene does not exhibit such a maximum corroborates this analysis. The preferred orientation of the linear C_2H_2 molecule at that distance is such that the symmetry axis of the guest lies parallel to the symmetry axis of the host, and thus C_2H_2 can slip through the cavity opening without encountering significant repulsive interactions with the *tert*-butyl hydrogens. (The difference between a C_2H_2 guest and a CO_2 guest when sequestered by TBC4 is particularly striking. The C_2H_2 guest lies "flat" within the cavity when bound but exits the cavity end-on; the CO_2 guest behaves in an exactly opposite way, lying on average along the host's symmetry axis when bound but exiting the cavity perpendicular to that axis. The origin of this difference, of course, lies in the opposite polarities of the outermost atoms of the two molecules, i.e., in the opposite signs of the guests' quadrupole moments.)

The final guest molecule considered in this work is methanol, which was shown to form stable complexes with the shallower-cavity calixarenes discussed previously. As expected, the dynamics of sequestered MeOH does not differ from what we found previously for the C4/MeOH complex; that is, the motion of MeOH within the cavity is such that the alcohol group hydrogen is preferentially directed toward an aryl ring center. Here, too, we find that complexation with MeOH damps the asymmetric breathing vibration of the host cavity and does so to the same extent as in C4. Thus, for all practical purposes, para substitution of methyl or *tert*-butyl groups for hydrogen has no effect on the binding or dynamics of MeOH within the cavity or on the effect that the guest has on the dynamics of the host. The interactions are strong enough in these systems that lengthening the host cavity is immaterial.

Calculating the potentials of mean force for the TBC4/MeOH system has provided us with an unexpected result, however. The free energy curve corresponding to 298 K, shown in Figure 12 (solid circles), is much like those reported for the C4/MeOH complex, but we find a qualitatively different distance dependence of the free energy at the lowest temperature, 100 K. To illustrate this point, we give in Figure 20 the free energy curves obtained at the same three temperatures considered previously.

The expected two minima in the binding free energy curve corresponding to orientations of the oxygen atom of methanol either toward the lower rim of the cavity (the minimum at smaller R) or toward the upper rim (the minimum at larger R) are clearly observed at 200 and 298 K, but only the latter minimum is found in simulations carried out at 100 K. To understand this difference, recall that when the methanol molecule "inverts" within the cavity, it does so to optimize the attractive interaction between the oxygen atom and the positively charged inner surface of the cavity near the lower rim. However, when it does so, the methyl group of the molecule necessarily must be oriented toward the upper cavity rim. In the C4/MeOH complex (and for MC4/MeOH as well), this reorientation of the methyl group does not yield appreciable repulsive interactions between the methyl hydrogens of the guest and the host's substituent groups. That repulsive interaction is stronger in the case of the *tert*-butyl substituents, though. Furthermore, at the higher temperatures, the large-amplitude thermal distortions of the host tend to mitigate this repulsive interaction, but the distortions characteristic of the lowest temperature are not able to do so. Thus, inversion of the methanol becomes increasingly energetically unfavorable as the temperature is lowered.

Because liquid methanol is frequently used as a solvent for the calix[4]arenes considered in the present work,[45] the apparent propensity of MeOH to bind to these hosts offers no particular surprise. Accordingly, we have selected this system for an evaluation of the correspondence between the dynamics of a host−guest complex and the dynamics of a host molecule in solution. The initial configuration for the simulation of TBC4 in liquid MeOH did not include a methanol molecule within the host cavity, but we found that a solvent molecule entered

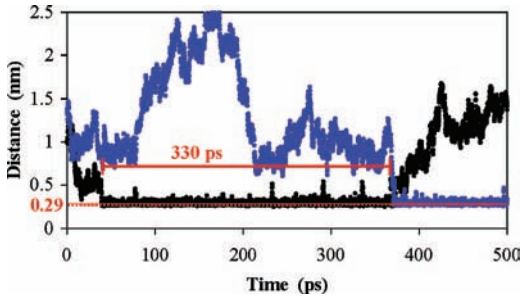

Figure 21. Oxygen−oxygen bond distance involving a methanol molecule sequestered in the TBC4 cavity at 298 K and a methanol solvent molecule found at the entrance to the cavity. The black and blue traces refer to different solvent molecules involved in hydrogen bonds with the guest.

the cavity during the initial NVT equilibration and that same molecule remained within the cavity throughout the equilibration sequences and the final collection of dynamics information. This sequestered MeOH is nearly indistinguishable dynamically from one forming a gas-phase complex with TBC4. The dynamics of the host molecule itself remains unchanged as well, a result leading us to conclude that perturbation of the breathing dynamics here is influenced primarily by the presence of the strongly bound guest rather than by the solvent molecules exterior to the host.

The persistence of a solvent molecule within the cavity over a time scale longer than that considered in this study would suggest that the sequestered methanol molecule does not communicate with the bulk solvent. (No evidence of exchange has been observed.) That conclusion is not entirely valid, however. When we follow the dynamics of the solvent molecule positioned at the upper rim of the host, just beyond the constriction created by the *tert*-butyl groups, we find that this solvent molecule forms a hydrogen bond with the sequestered methanol molecule and that this interaction survives for hundreds of picoseconds. To illustrate our point, we show in Figure 21 a plot of the oxygen−oxygen distance for the guest and two particular solvent molecules.

For both solvent molecules shown, the average oxygen−oxygen distance is 0.29 nm during the periods when they interact strongly with the MeOH guest molecule, a distance consistent with that reported for the MeOH dimer. This interaction does have the effect of keeping the sequestered guest oriented with its oxygen atom lying in the direction of the upper rim of the TBC4 host and preventing the occasional end-over-end inversions depicted in Figure 6. Clearly, therefore, the sequestered guest molecule does communicate with the bulk solvent, not to the extent that solvent exchange is rapid, but rather through hydrogen bond formation in which a solvent molecule lying in the cavity opening interacts with the exposed oxygen of the guest. The OH hydrogen of the guest meanwhile retains its interaction with the aryl rings of the host.

V. Conclusions

In the present study, we have used molecular dynamics simulations to examine the dynamics of host−guest complexes involving calix[4]arenes and small gas molecules and to correlate the dynamics with thermodynamic quantities relevant to the reaction coordinate for loss of the guests from the host cavities. Our long-range goal in this work is to shed light on the unexpected porosity of the low-density β_0 crystal polymorph of *p-tert*-butylcalix[4]arene, a material that has been shown to sorb gases at levels consistent with the occupation of large fractions of the available host cavity binding sites. Several dynamical characteristics of the host calixarenes are common to the systems examined here: the hydrogen bond network at the lower rim is quite rigid; the large-amplitude, low-frequency asymmetric breathing motion of the aryl rings leads to significant distortion of the shape of the host cavity; methyl and *tert*-butyl upper-rim substituents rotate quite freely, behavior consistent with the gating hypothesized in explanation of the ease with which gases enter the solid-state host cavities; and both the asymmetric breathing motion and the substitutent rotation of the host are preserved (although the breathing is somewhat damped) upon binding a small gas molecule within its cavity. Also common to these species is the band of negative charge density that rings the inner surface of the host cavity. The interactions of guest molecules with this charge distribution ultimately determines the stabilities of the resulting host−guest complexes, the equilibrium binding geometries, and the dynamics of the guests relative to their equilibrium binding orientations.

In all the cases in which small guest molecules form stable complexes with calixarene hosts at room temperature, the guests are oriented in such a way that their center (or centers) of positive charge density are in close proximity to the centers of negative charge density in the hosts, that is, at the centers of the aryl rings. For those complexes that are found to be unstable at room temperature, the geometry of the host cavity is such that some of the interactions with the guest are relatively unfavorable, a situation that promotes frequent transitions between equivalent binding orientations. Thermal motion of these species is then sufficient to lead to loss of the guests entirely. Carbon dioxide, the only guest considered in which the host−guest interactions do not reflect hydrogen bonding to the aryl ring π-electrons, is also found to be stabilized by elongation of the host cavity and by constriction of the cavity entrance. Finally, we have found a close correspondence between the dynamics of a methanol molecule complexed with TBC4 and the dynamics of a methanol molecule sequestered by TBC4 upon solvation in liquid methanol. The sequestered methanol does not exchange with bulk solvent over the time scale of our simulations, but it does perturb the motion of the solvent molecule that lies just beyond the cavity entrance. This particular solvent molecule forms a hydrogen bond with the guest and exchanges with other bulk molecules only on a time scale of hundreds of picoseconds.

Our results suggest that the formation of a stable host−guest complex is only a part of the answer to the question of why low-density TBC4 sorbs gases readily. While the structural fluctuations of the host and the stability of a complex with CO_2 is consistent with the observed uptake of gas by the crystal, the uptake of methane and acetylene is also well documented. The next issue to address, then, is how the dynamics and stability of complexes involving gas-phase hosts differ from those formed when the hosts are spatially confined as they are in the solid state. To address this issue, we are examining in detail the dynamics of tethered host dimers. The results of this extension of the present work will be presented in a separate report.

Acknowledgment. We thank Prof. Jerry Atwood and Drs. Scott Dalgarno and Nicholas Power for helpful discussions concerning this work.

References and Notes

(1) Atwood, J. L.; Barbour, L. J.; Jerga, A.; Schottel, B. L. *Science* **2002**, *298*, 1000–1002.

(2) Atwood, J. L.; Barbour, L. J.; Jerga, A. *Angew. Chem., Int. Ed.* **2004**, *43*, 2948–2950.

(3) Atwood, J. L.; Barbour, L. J.; Thallapally, P. K.; Wirsig, T. B. *Chem. Commun.* **2005**, 51–53.
(4) Thallapally, P. K.; Lloyd, G. O.; Wirsig, T. B.; Bredenkamp, M. W.; Atwood, J. L.; Barbour, L. J. *Chem. Commun.* **2005**, 5272–5274.
(5) Thallapally, P. K.; Wirsig, T. B.; Barbour, L. J.; Atwood, J. L. *Chem. Commun.* **2005**, 4420–4422.
(6) Thallapally, P. K.; Dobrzanska, L.; Gingrich, T. R.; Wirsig, T. B.; Barbour, L. J.; Atwood, J. L. *Angew. Chem., Int. Ed.* **2006**, *45*, 6506–6509.
(7) Thallapally, P. K.; Dalgarno, S. J.; Atwood, J. L. *J. Am. Chem. Soc.* **2006**, *128*, 15060–15061.
(8) Thallapally, P. K.; Kirby, K. A.; Atwood, J. L. *New J. Chem.* **2007**, *31*, 628–630.
(9) Thallapally, P. K.; McGrail, B. P.; Atwood, J. L. *Chem. Commun.* **2007**, 1521–1523.
(10) Dalgarno, S. J.; Thallapally, P. K.; Barbour, L. J.; Atwood, J. L. *Chem. Soc. Rev.* **2007**, *36*, 236–245.
(11) Atwood, J. L., Barbour, L. J., Jerga, A. Method of separating and storing volatile gases; (The Curators of the University of Missouri Office of Technology and Special Projects, USA). Application: WO, 2006; 32 pp.
(12) Enright, G. D.; Udachin, K. A.; Ripmeester, J. A. *Chem. Commun.* **2004**, 1360–1361.
(13) Brouwer, E. B.; Enright, G. D.; Udachin, K. A.; Lang, S.; Ooms, K. J.; Halchuk, P. A.; Ripmeester, J. A. *Chem. Commun.* **2003**, 1416–1417.
(14) Atwood, J. L.; Barbour, L. J.; Lloyd, G. O.; Thallapally, P. K. *Chem. Commun.* **2004**, 922–923.
(15) Ripmeester, J. A.; Enright, G. D.; Ratcliffe, C. I.; Udachin, K. A.; Moudrakovski, I. L. *Chem. Commun.* **2006**, 4986–4996.
(16) Atwood, J. L.; Barbour, L. J.; Jerga, A. *Chem. Commun.* **2002**, 2952–2953.
(17) Udachin, K. A.; Enright, G. D.; Ratcliffe, C. I.; Ripmeester, J. A. *ChemPhysChem* **2003**, *4*, 1059–1064.
(18) Ananchenko, G. S.; Udachin, K. A.; Pojarova, M.; Jebors, S.; Coleman, A. W.; Ripmeester, J. A. *Chem. Commun.* **2007**, 707–709.
(19) Ghoufi, A.; Bonal, C.; Morel, J. P.; Morel-Desrosiers, N.; Malfreyt, P. *J. Phys. Chem. B* **2004**, *108*, 5095–5104.
(20) Ghoufi, A.; Morel, J. P.; Morel-Desrosiers, N.; Malfreyt, P. *J. Phys. Chem. B* **2005**, *109*, 23579–23587.
(21) Ghoufi, A.; Pison, L.; Morel, J. P.; Morel-Desrosiers, N.; Bonal, C.; Malfreyt, P. *J. Phys. Chem. B* **2007**, *111*, 11478–11485.
(22) Lang, J.; Deckerova, V.; Czernek, J.; Lhotak, P. *J. Chem. Phys.* **2005**, *122*, 044506/044501–044506/044511.
(23) Leon, S.; Leigh, D. A.; Zerbetto, F. *Chem.−Eur. J.* **2002**, *8*, 4854–4866.
(24) Zanuy, D.; Casanovas, J.; Aleman, C. *J. Phys. Chem. B* **2006**, *110*, 9876–9881.
(25) Broda, F.; Vysotsky, M. O.; Boehmer, V.; Thondorf, I. *Org. Biomol. Chem.* **2006**, *4*, 2424–2432.
(26) Kawaguchi, T.; Ohki, H.; Yamada, K.; Okuda, T.; Haino, T.; Fukazawa, Y. *J. Mol. Struct.* **2007**, *833*, 108–113.
(27) Den Otter, W. K.; Briels, W. J. *J. Am. Chem. Soc.* **1998**, *120*, 13167–13175.
(28) Tolpekina, T. V.; Den Otter, W. K.; Briels, W. J. *J. Phys. Chem. B* **2003**, *107*, 14476–14485.
(29) Wipff, G. *Book of Abstracts, 217th ACS National Meeting, Anaheim, Calif., March 21−25* **1999**, I&EC−227.
(30) Wipff, G. *Calixarenes* **2001**, *2001*, 312–333.
(31) Wipff, G.; Engler, E.; Guilbaud, P.; Lauterbach, M.; Troxler, L.; Varnek, A. *New J. Chem.* **1996**, *20*, 403–417.
(32) Varnek, A.; Sirlin, C.; Wipff, G. *NATO ASI Ser., Ser. C* **1996**, *480*, 67–99.
(33) Varnek, A.; Volkova, T.; Petrukhin, O. M.; Wipff, G. *J. Inclusion Phenom. Macrocycl. Chem.* **2000**, *37*, 407–421.
(34) Varnek, A.; Wipff, G.; Famulari, A.; Raimondi, M.; Vorob'eva, T.; Stoyanov, E. *J.Chem. Soc., Perkin Trans. 2* **2002**, 887–893.
(35) Varnek, A.; Wipff, G.; Solov'ev, V. P.; Solotnov, A. F. *J. Chem. Inf. Comput. Sci.* **2002**, *42*, 812–829.
(36) Ghoufi, A.; Archirel, P.; Morel, J.-P.; Morel-Desrosiers, N.; Boutin, A.; Malfreyt, P. *ChemPhysChem* **2007**, *8*, 1648–1656.
(37) Ghoufi, A.; Bonal, C.; Morel, J. P.; Morel-Desrosiers, N.; Malfreyt, P. *J. Phys. Chem. B* **2004**, *108*, 11744–11752.
(38) Ghoufi, A.; Malfreyt, P. *Mol. Phys.* **2006**, *104*, 3787–3799.
(39) Ghoufi, A.; Malfreyt, P. *J. Chem. Phys.* **2006**, *125*, 224503/224501–224503/224512.
(40) Ghoufi, A.; Malfreyt, P. *Mol. Phys.* **2006**, *104*, 2929–2943.
(41) Raymo, F. M.; Bartberger, M. D.; Houk, K. N.; Stoddart, J. F. *J. Am. Chem. Soc.* **2001**, *123*, 9264–9267.
(42) Daschbach, J. L.; Thallapally, P. K.; Atwood, J. L.; McGrail, B. P.; Dang, L. X. *J. Chem. Phys.* **2007**, *127*, 104703/104701–104703/104704.
(43) Alavi, S.; Afagh, N. A.; Ripmeester, J. A.; Thompson, D. L. *Chem.−Eur. J.* **2006**, *12*, 5231–5237.
(44) Alavi, S.; Ripmeester, J. A. *Chem.−Eur. J.* **2008**, *14*, 1965–1971.
(45) de Namor, A. F. D.; Cleverley, R. M.; Zapata-Ormachea, M. L. *Chem. Rev.* **1998**, *98*, 2495–2525.
(46) Case, D. A.; Darden, T. A.; Cheatham, T. E., III; Simmerling, C. L.; Wang, J.; Duke, R. E.; Luo, R.; Merz, K. M.; Pearlman, D. A.; Crowley, M.; Walker, R. C.; Zhang, W.; Wang, B.; Hayik, S.; Roitberg, A.; Seabra, G.; Wong, K. F.; Paesani, F.; Wu, X.; Brozell, S.; Tsui, V.; Gohlke, H.; Yang, L.; Tan, C.; Mongan, J.; Hornak, V.; Cui, G.; Beroza, P.; Mathews, D. H.; Schafmeister, C.; Ross, W. S.; Kollman, P. A. *AMBER 9*; University of California: San Francisco, 2006.
(47) Cornell, W. D.; Cieplak, P.; Bayly, C. I.; Gould, I. R.; Merz, K. M., Jr.; Ferguson, D. M.; Spellmeyer, D. C.; Fox, T.; Caldwell, J. W.; Kollman, P. A. *J. Am. Chem. Soc.* **1995**, *117*, 5179–5197.
(48) Cornell, W. D.; Cieplak, P.; Bayly, C. I.; Gould, I. R.; Merz, K. M., Jr.; Ferguson, D. M.; Spellmeyer, D. C.; Fox, T.; Caldwell, J. W.; Kollman, P. A. *J. Am. Chem. Soc.* **1996**, *118*, 2309.
(49) Wang, J.; Wolf, R. M.; Caldwell, J. W.; Kollman, P. A.; Case, D. A. *J. Comput. Chem.* **2004**, *25*, 1157–1174.
(50) Wang, J.; Wolf, R. M.; Caldwell, J. W.; Kollman, P. A.; Case, D. A. *J. Comput. Chem.* **2004**, *26*, 114.
(51) Duan, Y.; Wu, C.; Chowdhury, S.; Lee, M. C.; Xiong, G.; Zhang, W.; Yang, R.; Cieplak, P.; Luo, R.; Lee, T.; Caldwell, J.; Wang, J.; Kollman, P. *J. Comput. Chem.* **2003**, *24*, 1999–2012.
(52) Ryckaert, J. P.; Ciccotti, G.; Berendsen, H. J. C. *J. Comput. Phys.* **1977**, *23*, 327–341.
(53) Bayly, C. I.; Cieplak, P.; Cornell, W.; Kollman, P. A. *J. Phys. Chem.* **1993**, *97*, 10269–10280.
(54) Cornell, W. D.; Cieplak, P.; Bayly, C. I.; Kollman, P. A. *J. Am. Chem. Soc.* **1993**, *115*, 9620–9631.
(55) Frisch, M. J.; Trucks, G. W.; Schlegel, H. B.; Scuseria, G. E.; Robb, M. A.; Cheeseman, J. R.; Montgomery, J., J. A.; Vreven, T.; Kudin, K. N.; Burant, J. C.; Millam, J. M.; Iyengar, S. S.; Tomasi, J.; Barone, V.; Mennucci, B.; Cossi, M.; Scalmani, G.; Rega, N.; Petersson, G. A.; Nakatsuji, H.; Hada, M.; Ehara, M.; Toyota, K.; Fukuda, R.; Hasegawa, J.; Ishida, M.; Nakajima, T.; Honda, Y.; Kitao, O.; Nakai, H.; Klene, M.; Li, X.; Knox, J. E.; Hratchian, H. P.; Cross, J. B.; Bakken, V.; Adamo, C.; Jaramillo, J.; Gomperts, R.; Stratmann, R. E.; Yazyev, O.; Austin, A. J.; Cammi, R.; Pomelli, C.; Ochterski, J. W.; Ayala, P. Y.; Morokuma, K.; Voth, G. A.; Salvador, P.; Dannenberg, J. J.; Zakrzewski, V. G.; Dapprich, S.; Daniels, A. D.; Strain, M. C.; Farkas, O.; Malick, D. K.; Rabuck, A. D.; Raghavachari, K.; Foresman, J. B.; Ortiz, J. V.; Cui, Q.; Baboul, A. G.; Clifford, S.; Cioslowski, J.; Stefanov, B. B.; Liu, G.; Liashenko, A.; Piskorz, P.; Komaromi, I.; Martin, R. L.; Fox, D. J.; Keith, T.; Al-Laham, M. A.; Peng, C. Y.; Nanayakkara, A.; Challacombe, M.; Gill, P. M. W.; Johnson, B.; Chen, W.; Wong, M. W.; Gonzalez, C.; Pople, J. A. *Gaussian 03, Revision D.01*; Gaussian, Inc.: Wallingford, CT, 2004.
(56) Izaguirre, J. A.; Catarello, D. P.; Wozniak, J. M.; Skeel, R. D. *J. Chem. Phys.* **2001**, *114*, 2090–2098.
(57) Darden, T.; York, D.; Pedersen, L. *J. Chem. Phys.* **1993**, *98*, 10089–10092.
(58) Essmann, U.; Perera, L.; Berkowitz, M. L.; Darden, T.; Lee, H.; Pedersen, L. G. *J. Chem. Phys.* **1995**, *103*, 8577–8593.
(59) NIST Chemistry Webbook. Thermophysical Properties of Fluid Systems. http://webbook.nist.gov/chemistry/fluid/(January 16, 2008).
(60) Kumar, S.; Rosenberg, J. M.; Bouzida, D.; Swendsen, R. H.; Kollman, P. A. *J. Comput. Chem.* **1995**, *16*, 1339–1350.
(61) Roux, B. *Comput. Phys. Commun.* **1995**, *91*, 275–282.
(62) Trzesniak, D.; Kunz, A.-P. E.; van Gunsteren, W. F. *ChemPhysChem* **2007**, *8*, 162–169.
(63) Grossfield, A. An implementation of WHAM: the weighted histogram analysis method, version 2.0.2, 2008.
(64) Dennington, II R.; Keith, T.; Millam, J.; Eppinnett, K.; Hovell, W. L.; Gilliland, R. *GaussView, version 3.09*; Semichem, Inc.: Shawnee Mission, KS, 2003.
(65) Graham, C.; Imrie, D. A.; Raab, R. E. *Mol. Phys.* **1998**, *93*, 49–56.
(66) Nowak, R.; Menapace, J. A.; Bernstein, E. R. *J. Chem. Phys.* **1988**, *89*, 1309–1321.
(67) Pribble, R. N.; Hagemeister, F. C.; Zwier, T. S. *J. Chem. Phys.* **1997**, *106*, 2145–2157.
(68) Boese, R.; Clark, T.; Gavezzotti, A. *Helv. Chim. Acta* **2003**, *86*, 1085–1100.

JP800492Y